Non-Linear Boundary Conditions for a Structure Under Fluid-Structure Interactions

K. Takeuchi, D. Bhandari

Westinghouse Electric Corporation, Nuclear Energy Systems, P.O. Box 355, Pittsburgh, Pennsylvania 15230, U.S.A.

Abstract

A method of solving structural dynamics with non-linear boundary condition in fluid-structural interactions is presented. It is incorporated into the advanced beam model of MULTIFLEX code. An analysis of a LOCA load on a 3-loop thermal shield plant is performed. Computed barrel-vessel relative displacements are shown to agree very well with those computed by WECAN code, verifying the present methodology.

1. Introduction

For a hypothetical PWR Loss-of-Coolant Accident (LOCA), acoustic wave fluid-structure interaction in the downcomer is important in evaluation of its consequences. For this purpose various computer codes have been developed; for example KFIX/FLX[1] and FLUX[2]. These codes are multi-dimensional codes developed to analyze HDR experiments[3]. MULTIFLEX code, on the other hand, is a one-dimensional code developed as an engineering tool to compute hydraulic loads on vessel supports as well as reactor internals. Although the code is one-dimensional a network can be constructed for multi-dimensional fluid-structure interactions[4].

The original fluid-structure interaction in the downcomer is to allow for the core barrel flexibility as represented by a beam model[5]. The flexible deformations of both the core barrel and vessel cylinders are then taken into account. This is formulated by the use of the relative modal analyses as shown in Reference 6. At the same time, a projector method has been developed to super-impose beam and shell modes without overlap[6,7].

Structural models in the above codes are linear. In a real PWR system, however, there exist mechanical non-linearities such as gaps in supporting flanges between the core barrel and the pressure vessel. Even after gap closure, the component stiffness is load dependent and hence is not constant mainly because the contact area between the flanges increases with the load. Furthermore, impact damping plays an important role in the dynamic response as the gaps are closed. Therefore, a method of dealing with the non-linear boundary conditions of structural model under fluid-structure interactions is developed as described below. A typical response of the PWR internals to a LOCA is analyzed.

In Section 2, hydraulic conservation equations and non-linear structural dynamic equations are given which identify the fluid-structure interaction terms. To solve the non-linear equations, the intermediate pseudo-force method is developed in Section 2.1, as a generalization of the pseudo force[8] modal superposition[9,10]. The modal analysis is further developed to a relative modal analysis for fluid-structure interactions in the co-axial cylinders. Section 2.2 briefly describes a hydraulic network model for a three loop thermal shield primary coolant system. In Section 3, two structural finite element models developed using WECAN code[10] are discussed. The one is a condensed linearized model to generate structural input data to MULTIFLEX. Another is a detailed dynamic structural model which uses hydraulic forces, post-processed from MULTIFLEX to compute structural response in terms of deformations, impact loads, forces and moments of the reactor pressure vessel and its internals. In Section 4, structural displacements computed by MULTIFLEX are compared with WECAN to verify the method of computation presented in the paper.

2. Mathematical Description for Fluid-Structure Interactions with Non-Linear Structural Boundary Conditions

In order to solve dynamic problems of fluid-structure interactions, one-dimensional hydraulic conservation equations together with structural equations of motion are solved in the MULTIFLEX code. The basic governing equations and their method of solution is briefly described below.

Mass conservation:

$$\frac{\partial}{\partial t}(\rho A) + \frac{\partial}{\partial z}(GA) = 0 \qquad (2\text{-}1)$$

Momentum conservation:

$$\frac{\partial}{\partial t}(GA) + \frac{\partial}{\partial z}(uGA) + \frac{\partial p}{\partial z} = -\rho FA \qquad (2\text{-}2)$$

Energy conservation:

$$\frac{\partial h}{\partial t} + u\frac{\partial h}{\partial z} - \frac{1}{\rho}\left(\frac{\partial p}{\partial t} + u\frac{\partial p}{\partial z}\right) = Q + uF \qquad (2\text{-}3)$$

Wherein the hydro-dynamic variables ρ, G, p and h are the density, mass flow rate, pressure and enthalpy, respectively; and u is the fluid velocity. The heat generation rate per unit mass is denoted by Q, and F stands for the frictional and gravitational contributions.

The flow area is a function of the structural deformation, vector [x], which is determined by the equation of structural motion,

$$\{M\}[\ddot{X}] + \{C([\dot{X}], [X])\} + \{K([X])\} = [f(p)] \qquad (2\text{-}4)$$

subjected to the hydraulic force [f(p)], where $\{M\}$, $\{C\}$, and $\{K\}$ are mass, damping and stiffness matrices, respectively. The hydraulic force is a function of pressure obtained from eqs. (2-1) - (2-3). On the other hand, these equations have terms of time derivative of flow area, A, which is a function of structural displacements, $\dot{A} = \dot{A}([X])$. Thus, eqs.

(2-1) - (2-4) are coupled for fluid-structure interactions.

2.1 Intermediate Pseudo-Force Method for Non-Linear Boundaries

Structural non-linearity in fluid-structure interactions[8] can be taken into account by the pseudo-force method that solves the structural dynamic equation with the non-linear terms incorporated in the external force term. Furthermore, time dependent modal analysis is demonstrated in References 9 and 10 to be capable of solving a structural non-linear boundary problem by the use of the pseudo-force method (known also as modal superposition). These methods are generalized in this section so as to include linearized boundary conditions in the modal analysis and the difference between the non-linear and the linearized boundary conditions in the pseudo-force term; the intermediate pseudo-force method.

The stiffness and damping matrices in eq. (2-4) are non-linear in terms of the displacement vector [X]. To solve eq. (2-4), these matrices are decomposed into linear and non-linear parts;

$$\{C([\dot{X}],[X])\} = \{C_\ell\}[\dot{X}] + \{C_{n\ell}([\dot{X}],[X])\} \tag{2-5}$$

$$\{K([X])\} = \{K_\ell\}[X] + \{K_{n\ell}([X])\} \tag{2-6}$$

$$= \{\overline{K}_\ell\}[X] + \{K_{n\ell}'([X])\} \tag{2-7}$$

In eq. (2-7), linearized stiffness matrix $\{\overline{K}_{n\ell}\}$ has been introduced; i.e.,

$$\{\overline{K}_\ell\} = \{K_\ell\} + \{\overline{K}_{n1}\} \tag{2-8}$$

and

$$\{K_{n\ell}'([X])\} = \{K_{n\ell}([X])\} - \{\overline{K}_{n\ell}\}[X] \tag{2-9}$$

Then, eq. (2-4) becomes,

$$\{M\}[\ddot{X}] + \{C_\ell\}[\dot{X}] + \{\overline{K}_\ell\}[X] = [\bar{F}(p)] - \{C_{n\ell}\}[\dot{X}] - \{K_{n\ell}'\}[X] \tag{2-10}$$

This equation is solved by the use of modal decomposition whose modes are solution of eq. (2-10) with vanishing r.h.s.

If the linearized boundary condition is chosen to be zero, $\{\overline{K}_{n\ell}\} = 0$, then eq. (2-10) becomes pseudo-force method in Reference 6, where spurious modes come out. The spurious modes can be avoided and optimization can be achieved by reasonably selected linearized stiffness matrix $\{\overline{K}_{n\ell}\}$. The obtained mode shapes are physically reasonable independent of initial gap open or close status.

Equation (2-10) can be solved through the modal analysis, wherein the eigen-value problem with linearized stiffness becomes;

$$\{M\}^{-1}\{\bar{K}_{\ell}\}\{\Phi\} = \{\Phi\}\{\Omega_o\}^2 \tag{2-11}$$

is solved for the mode shape matrices $\{\Phi\}$ and the in-air frequency $\{\Omega_o\}$. Then, the generalized mass matrix is computed,

$$\{M^*\} = \{\Phi\}^T\{M\}\{\Phi\} \tag{2-12}$$

Now that the structural displacement is related to the generalized coordinate [q] by

$$[X] = \{\Phi\}[q] \tag{2-13}$$

Equation (2-10) becomes

$$[\ddot{q}] + 2\eta\{\Omega_o\}[\dot{q}] + \{\Omega_o\}^2[q] = \{M^*\}^{-1}\{\Phi\}^T([F] + [N]), \tag{2-14}$$

where the non-linear pseudo-force is

$$[N] = -\{C_{n\ell}\}[\dot{X}] - \{K_{n\ell}'\}[X] \tag{2-15}$$

For the chosen linearized stiffness $\bar{K}_{n\ell}$, the pseudo-force becomes

$$N = \bar{K}_{n\ell}\, r_N - \begin{cases} K_{n\ell}(r_N - g) + C_{n\ell}\dot{r}_N & \text{for } r_N > g \\ K_{n\ell}(r_N + g) + C_{n\ell}\dot{r}_N & \text{for } r_N < -g \\ 0 & \text{otherwise} \end{cases} \tag{2-16}$$

where r_N is the relative displacement between the barrel and the vessel at a particular boundary point, for concentric gaps.

It is now straight forward to follow the procedure in References 7 and 8 to transform the absolute displacement [X] in eq. (2-13) to the relative displacement [r] and the center of mass displacement [R]. As a result, eq. (2-14) for [q] becomes the same expression but $[\Phi]$ being replaced by the relative mode shape $[\psi_r]$.

2.2 Thermal-Hydraulic Model for a PWR Primary System

The above method of advanced beam model is applied to a postulated LOCA of a limited break at a cold leg inlet nozzle of a three-loop thermal shield plant. The entire primary system is modeled in MULTIFLEX computation. Two of the unbroken intact loops are lumped into one model loop with a steam generator and a pump. A broken loop is separately modeled with a break model attached. It is usual to assume that the loop with pressurizer is broken. The reactor internals are modeled also in detail with the network downcomer model. A steady state computation is performed to obtain a balanced heat, pressure, and flow rate distribution, which is not a trivial task by itself but of importance to the results of transient computation.

A transient is initiated with the break model opening the pipe to the containment via the postulated maximum break area with 1 ft^2. Then depressurization wave propagates towards the downcomer. Within 5 msec or so into the transient, the core barrel begins to vibrate and re-shape the pressure field in the downcomer. This fluid-structure interaction is the most important effect in the LOCA of the other types such as pipe deformation, elbow elongation, and deformation of the other components in the reactor internals. This is the reason for extensive study performed in this area of fluid-structure interactions[1-6].

The downcomer annulus is basically 2-dimensional fluid system with fluid-structure interactions 1-D equivalent to which network formation is developed in Reference 4. The rules for the network formation are:

(1) The flow area of an axial leg is equal to the flow area of the circumferential leg.

(2) The sonic velocity in the network legs is multiplied by $\sqrt{2}$.

(3) The force term in Equation (2-34) is multiplied by 1/2.

Rules 2 and 3 are incorporated in the code and rule 1 is taken care of in the modeling.

Variations of rule number 1 are studied in References 6 and 7 because the annulus configuration of a real reactor is not so simple as the development model[4]. The location of the inlet-nozzle and consideration of pressure wave penetration affect the choice of network mesh size and flow area as well. Furthermore, the thickness of annulus varies around the barrel-vessel flanges, below the inlet nozzle downcomer joint, and at the elevation of thermal shield. Especially, the thermal shield makes the downcomer a double annuli configuration. Correspondingly, a doubly layered network is modeled, however, fluid-structure interaction of the inner annulus is found to be negligible.

Computed results from MULTIFLEX are the core barrel and vessel displacements and the pressure field in the downcomer among other hydraulic data in the reactor internals as well as in the external loops. From them, it is straight forward to compute MULTIFLEX barrel-vessel relative displacements. However, the normal procedure is to compute the hydraulic forces on the barrel and the vessel from the MULTIFLEX pressure field in the downcomer. These hydraulic forces are then applied to WECAN code with much more detailed structural model than MULTIFLEX so that stress computations on components can be performed. It is worth while to compare relative displacements computed by WECAN code with MULTIFLEX and this comparison is done in Section 4.

3. Structural Models

In evaluation of structural consequences of a LOCA, two structural models are used. The one is a condensed linearized model to obtain structural input data to MULTIFLEX as discussed in Section 3.1. The linearization is of course applied only to boundaries connecting different structural components. In Section 3.2, major structural joints in the reactor vessel are discussed and then represented by non-linear boundary conditions to be used for MULTIFLEX computations. The hydraulic forces computed by MULTIFLEX are then applied to the second structural model. The second model is a detailed 3-D model for WECAN code to compute structural response in terms of deformations, impact loads, forces and moments of the pressure vessel and its internals.

3.1 Structural Input Data by Relative Modal Analysis

The structural input data required for MULTIFLEX consists of generalized masses, eigenfrequencies, relative mode shapes, weighted and non-weighted relative boundary shapes, and data of non-linear boundary conditions and linearized conditions. This input data is generalized using WECAN(10), a general purpose finite-element code. The system finite-element representation of a typical PWR and its internals for the normal mode analysis is shown in Fig. 3-1. Here, the core barrel, thermal shield and the reactor vessel are represented by concentric pipes (STIF7). The fuel assemblies are represented by 3-D beams; the upper support assembly consisting of guide tubes upper support columns and the deep beam is represented by mass and stiffness matrices (STIF27) obtained via substructuring technique. Note that this is a 3-D model with an artificially chosen linearized springs between nodes 4-11, 2-5, 5-15, and 6-16. Applied to this model is the normal mode analysis, condensing all the dynamic degrees of freedom other than linear displacement in the X-Z plane, and rotation around Z-axis.

Then, the relative mode shape ψ_r is computed from the weighted difference of the core barrel and vessel modal displacements.

3.2 Non-Linear Vessel-Barrel Boundary Conditions

In order to accommodate thermal expansions of the reactor internals and the vessel, design clearances are provided at the vessel/internals interfaces which introduce mechanical non-linearities at the boundaries. Typical radial clearances between the reactor vessel and the upper and lower internals is shown in Figure 3-2. The top non-linear boundary at the downcomer annulus is comprised of the barrel flange and the vessel flange. The size of the gap g at this boundary varies depending on the type and design configuration of the plant.

As the relative distance between the barrel and vessel flanges increases beyond the gap, the two flanges deform and the surface area in contact increases. Consequently, the force-displacement relation becomes nonlinear even after the gap is closed, as shown in Fig. 3-3.

The bottom boundary supports for the core barrel and the reactor vessel are at the lower radial key restraints. The force-displacement relationship for this boundary condition is shown in Fig. 3-4. In Fig. 3-4, line OA represents the elastic deformation and A the limit load capacity of two side keys after the tangential gap between the keys and clevis is closed. Slope AB represents the yielding of these two side keys till the third key comes in contact at point B. Lines BC and CD define, respectively, the limit load capacity and yielding of the third key.

3.3 Non-Linear System Structural Model

The computed hydraulic forces from the MULTIFLEX code are then used to calculate time-history response of the reactor pressure vessel and its internals. The non-linear system structural model used in this analysis is identical to the one used in normal mode analysis (see, e.q. Fig. 3-1) except that the linearized springs are replaced by non-linear springs (STIF37). From the system analysis the component stress resultants (moments and forces), interface impact forces and the deformations are calculated during LOCA transients.

4. Results of Computation

The MULTIFLEX method of solving structural dynamics presented in Section 2 is substantially simpler and different from WECAN. It is therefore worth while comparing structural deformation computed by these two codes. This provides us with a cross-code verification and a consistency proof of the procedure: The hydraulic forces are computed by MULTIFLEX with only a downcomer structural model that is the minimum required for fluid-structure interactions. The computed hydraulic forces are then applied to a detailed WECAN structural model of the entire primary system to evaluate the structural consequences of LOCA.

Shown in Fig. 4-1 and 4-2 are displacements of core barrel relative to the vessel computed by MULTIFLEX (solid curves) and by WECAN (dotted curves). Figure 4-1 is the relative displacement at the elevation of the top node in the downcomer that is fairly close to the vessel-barrel flanges. Time is scaled to the frequency of the barrel oscillation and the displacement is scaled to gap size g in Fig. 4-1. Similarly, Fig. 4-2 shows the relative displacement at the middle elevation of the thermal shield. Good agreement between MULTIFLEX and WECAN results can be seen.

5. Conclusion

The advanced beam model of MULTIFLEX consists of various methodologies: The relative modal analysis is to take into account the vessel motion in addition to the core-barrel motion. The three rules in Section 2.2 is to construct a 1-D network equivalent to 2-D fluid-structure interactions. Among these rules, rule 1 has been subjected to variations due to deviation of real downcomer configuration from the ideal one, see References 7 and 8. In the present case, a more drastic variation is experienced by the presence of the thermal shield.

In a real PWR, large gaps may exist at barrel-vessel flanges and bottom keys. To deal with such a large gap, conventional linearization may not adequately represent real situations. For this reason, the intermediate pseudo-force method is presented in the present paper. Contrary to the conventional modal superposition, the present intermediate pseudo-force method does not generate a spurious mode, such as rigid body motions.

Despite a significant difference of MULTIFLEX methodology and model from WECAN, computed results of barrel-vessel relative displacements agree very well. This verifies the present MULTIFLEX method of the advanced beam model.

6. References

1. W.C. Rivard, et. al., "Pre- and Post-Test Analyses with K-FIX for an HDR Blowdown Test", Nucl. Eng. and Design 70 (1982) 309.

2. A. Ludwig and U. Schuman, "Fluid-Structure Analysis for the HDR Blowdown and Snapback Experiments with FLUX", Nucl. Eng. and Design 70 (1982) 321.

3. L. Wolf, "Experimental Results of Coupled Fluid-Structure Interacting During Blowdown of the HDR - Vessel and Comparisons with Pre- and Post-Test Predictions", Nucl. Enq. and Design 70 (1982) 269.

4. K. Takeuchi, "One-Dimensional Network for Multi-Dimensional Fluid-Structure Interactions" Nucl. Sci. and Eng. 72 (1979) 322.

5. K. Takeuchi, D. J. Kowalski, V. J. Esposito, and F. M. Bordelon, "MULTIFLEX, A FORTRAN-IV Computer Program for Analyzing Thermal-Hydraulic Structural System Dynamics", WCAP-8708 (1976).

6. K. Takeuchi, "Analysis of HDR Blowdown Experiment for Fluid-Structure Interactions with MULTIFLEX", Nucl. Eng. and Design 70 (1982) 357.

7. K. Takeuchi and D. F. DeSanto, "Experiment and Analysis of Shell Model In-Water Frequencies of a 1/24th Scale Core Barrel Model", Nucl. Eng. and Design 59 (1980) 339.

8. K. Takeuchi, "Dynamic Pressure Wave Propagation in a Plastically Deforming Pipe", ANS to 26 (1977) 360.

9. A. J. Molnar, et. al., "Application of Normal Mode Theory and Pseudo-Force Methods to Solve Problems with Non-Linearities", J. of Pressure Vessel Tech. 98 (1976) 151.

10. WECAN, Westinghouse Electric Computer Analysis User's Manual, Vol. 1 and 2 (December 1976).

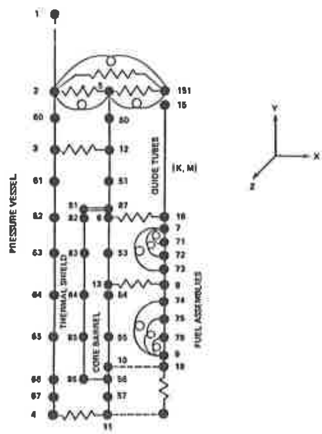

FIGURE 3-1 3D LINEARIZED SYSTEM MODEL OF VESSEL AND INTERNALS

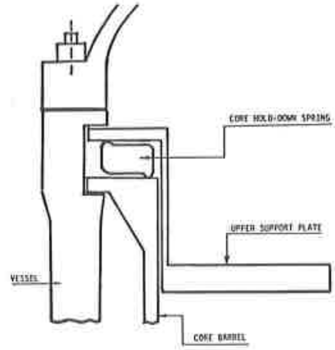

FIGURE 3-2 VESSEL/BARREL FLANGE REGION

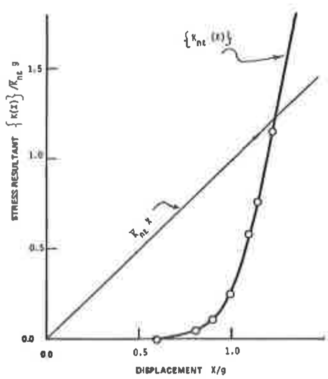

FIGURE 3-3 FORCE DISPLACEMENT RELATION AT BARREL

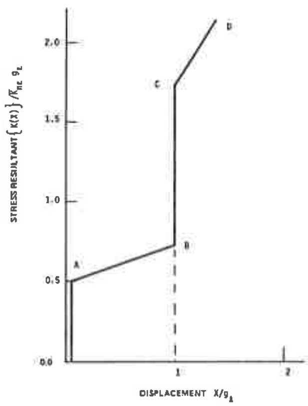

FIGURE 3-4 FORCE-DISPLACEMENT RELATION AT THE CORE SUPPORT PLATE

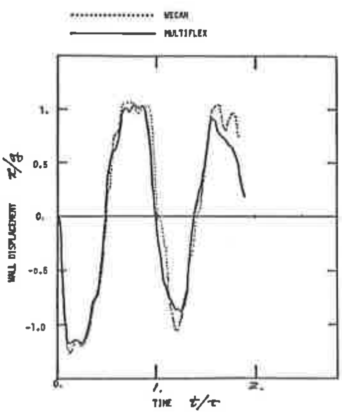

FIGURE 4-1 BARREL/VESSEL RELATIVE DISPLACEMENTS AT THE TOP LEVEL

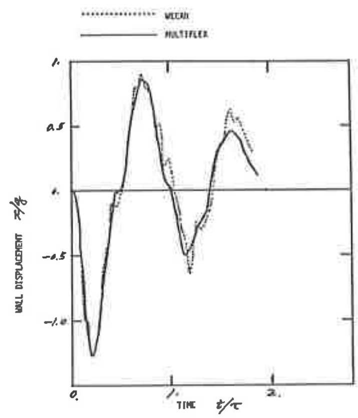

FIGURE 4-2 THERMAL SHIELD/VESSEL RELATIVE DISPLACEMENTS AT THE T.S. MIDDLE ELEVATION